Journal Pre-proofs

A new methodology to assess the solubility of fatty acids: Impact of food emulsifiers

Julieta N. Naso, Fernando A. Bellesi, Víctor M. Pizones Ruiz-Henestrosa, Ana M. R. Pilosof

PII: S0963-9969(20)30854-1
DOI: https://doi.org/10.1016/j.foodres.2020.109829
Reference: FRIN 109829

To appear in: *Food Research International*

Received Date: 19 June 2020
Revised Date: 14 October 2020
Accepted Date: 16 October 2020

Please cite this article as: Naso, J.N., Bellesi, F.A., Pizones Ruiz-Henestrosa, V.M., M. R. Pilosof, A., A new methodology to assess the solubility of fatty acids: Impact of food emulsifiers, *Food Research International* (2020), doi: https://doi.org/10.1016/j.foodres.2020.109829

A new methodology to assess the solubility of fatty acids: Impact of food emulsifiers.

Julieta N. Naso[1,2], Fernando A. Bellesi[1,3], Víctor M. Pizones Ruiz-Henestrosa[1,3] and Ana M. R. Pilosof[1,3]

(1) ITAPROQ- Departamento de Industrias, Facultad de Ciencias Exactas y Naturales, Universidad de Buenos Aires, Ciudad Universitaria (1428), Buenos Aires, Argentina.

(2) Fellowship Agencia Nacional de Promoción Científica y Tecnológica, Argentina.

(3) Consejo Nacional de Investigaciones Científicas y Técnicas (CONICET), Argentina.

* Corresponding author: A. M. R. Pilosof.

E-mail address: apilosof@di.fcen.uba.ar

Abstract

In food formulations, lipids are normally incorporated as emulsions stabilized by different types of emulsifiers. The emulsifiers can affect fatty acid (FA) solubilization as they can interact with FA. The main purpose of the present work is the development of a methodology to evaluate the FA solubilization in an aqueous medium in the absence and presence of exogenous emulsifiers.To this end, a combination of turbidimetry, oiling off and dynamic light scattering (DLS) was used. The FA solubility, as well as its supramolecular assemblies, were determined by analyzing the changes in the turbidity profile and the corresponding size of particles obtained by DLS. Oleic acid (OA) was used as a model FA and a simulated intestinal fluid (SIF) as the aqueous phase. Emulsifiers of low (Tween 80) and high (protein and polysaccharide) molecular weight were tested. Tween 80 was the only emulsifier that improved OA solubilization, whereas the macromolecules only affected the supramolecular structure that OA adopted, being the structure of these assemblies governed by the emulsifier nature.

KEYWORDS

Fatty acids, Solubility, Turbidity, DLS,Structure, Emulsifiers

1. Introduction

Medium- and long-chain fatty acids (FA) have a very low solubility in water at neutral pH. However, FA can be solubilized in micellar solutions of surfactants by incorporating in the formed mixed micelles. Tzocheva et al.(2012) reported that saturated straight-chain FA with n = 10 to 18 carbon atoms increased their solubility in micellar solutions of the anionic surfactant sodium laurylethersulfate and the zwitterionic surfactant cocamidopropylbetaine. The latter can serve as carriers of FA molecules during the processes of adsorption and formation of disperse systems (foams, emulsions, and suspensions). The adsorption or solubilization of fatty acids can essentially influence the interfacial properties, as well as the stability and rheology of dispersions. Mirgorodskaya, Yatskevich, & Zakharova (2010) studied the solubilization of FA in systems based on block copolymers and non-ionic surfactants extensively used in pharmaceutical practice. They found that the system based on surfactant that could form micelles (Tyloxapol, Triton-X-100 and Brij-97) increase the solubility of FA by more than an order of magnitude compared with water because of the formation of mixed aggregates. It seems that the FA molecules were incorporated into the micelles structure, increasing their size and provoking morphological changes. In contrast, the solutions that contained block copolymers (Pluronic F-127 and Synperonic F-68), that do not form micelles, had a weak effect on the FA solubility. However, in all the systems, the solubilization of the FA is accompanied by the partial or complete destruction of the intrinsic FA aggregates and a substantial decrease in the acid properties.

FA solubilization plays also a determinant role in the uptake of dietary lipids. During the lipolysis the triglycerides are transformed into monoglycerides and FA (Sarkar, Ye, & Singh, 2016). These products are solubilized into mixed bile salts and phospholipids micelles to facilitate their absorption (Maldonado-Valderrama, Wilde, MacIerzanka, & MacKie, 2011; Parker, Rigby, Ridout, Gunning, & Wilde, 2014). Only few studies have investigated this phenomenon using complex and not easy to reproduce methodologies (Freeman, 1969; Hofmann, 1963; Smith & Lough, 1976; Verkade & Meerburg, 1955).

Lipids are normally incorporated into food formulations as emulsions (mainly oil in water) or as foams, stabilized by surface active molecules of different nature, as low molecular weight emulsifiers (Tweens, lecithins, etc) or biopolymers as proteins or specific polysaccharides. These surfactants can interact with FA thus affecting their solubilization.

The main purpose of the present work is the development of a methodology that can be used to evaluate the water solubility of FA as affected by typical food emulsifiers. A synthetic and non-ionic emulsifier, Polysorbate 80 (commercially known as Tween 80), was tested as a common low molecular weight emulsifier; β-lactoglobulin, a widely used milk protein, and hydroxypropylmethylcellulose (HPMC), a surface active polysaccharide, as high molecular weight emulsifiers.

The concept of “solubilization” is used in this work in a broader meaning, as to maintain the FA in the aqueous phase, where different supramolecular structures can be adopted by the FA. To this end, a combination of turbidimetry, oiling off determination and dynamic light scattering (DLS) was used. The latter provided information about supramolecular assemblies occurring up to the limit of FA solubilization.

Solubility depends mainly on the carbon chain length of FA as well as on the degree of unsaturation, decreasing with increasing the length and saturation of carbon chain. Oleic acid (OA), that is one of the main FA forming dietary triglycerides, was used in this work as a model FA. It has been reported that, when dispersed in water, OA can adopt different supramolecular structures including micelles, bilayer vesicles or oil droplets, depending on the pH of the aqueous medium; at neutral pH OA spontaneously assemble into vesicles (Cistola, Hamilton, Jackson, & Small, 1988; de Kruijff et al., 2010; Small, 1986). Vesicles are self-closed structures formed by a curved amphiphile bilayer, mostly spherical in shape, that entraps a certain volume of the surrounding aqueous medium (Rasi, 2003).

From a chemical structure point of view, FA are amphiphilic molecules that contain an aliphatic tail and a polar head group that can be presented in its protonated (-COOH) or deprotonated ($-COO^-$) state, depending on the pH of the medium. By changing the protonation/ionization ratio of the carboxylic acid, a wide range of OA self-assembled structures can be reversibly obtained. When increasing the pH (pH>8-8.5) a higher ionized/protonated ratio is reached and micelles are the dominant supramolecular structure; however, when decreasing the pH (pH<8-8.5), less regular supramolecular structures, like droplets, are obtained due to a higher ratio of protonated to ionized molecules (Chen & Szostak, 2004; Cistola et al., 1988; Shu et al., 2014; Small, 1986). However, it has been suggested that the transition between the different structural states of OA (vesicles, micelles and droplets) at pH above and below the apparent pKa (8-8.5), is a complex transition involving regions of phase coexistence. This means that vesicles could coexist with the other states (micelles and droplets) at pH near

122 the apparent pKa (Rendón et al., 2012; Walde, Namani, Morigaki, & Hauser,
123 2010).

124 **2. Materials and methods**

125 **2.1 Materials**

126 Oleic acid (OA) was supplied by Quimica Mega (Argentina). Tween 80 (T80),
127 of analytical grade, was purchased from Biopack. BioPURE β-lactoglobulin (βlg)
128 was obtained from DAVISCO Foods International, Inc. (Le Sueur, Minnesota)
129 with a protein composition (dry basis) of 97.8%, being β-lactoglobulin 93.6% of
130 total proteins. Methocell (food grade) HPMC E5LV® from the Dow Chemical
131 company was kindly supplied by Colorcon (Argentina) and used without
132 purification. The characteristics of this HPMC were indicated previously by
133 Camino, Sánchez, Rodríguez Patino, & Pilosof (2011).

134 **2.2 Aqueous solutions preparation**

135 The emulsifiers were prepared at 0.5% w/w by dissolving them in a solution
136 that mimics the ionic composition and pH of duodenal fluid (39 mM K_2HPO_4, 150
137 mM NaCl and 30 mM $CaCl_2$ and pH 7) previously reported by Bellesi, Pizones
138 Ruiz-Henestrosa, & Pilosof (2014). The protein (βlg) and the nonionic surfactant
139 (T80) were easily dissolved by gently stirring. HPMC solutions were prepared by
140 dispersing the powder in SIF at 90ºC, and after that, cooled down to room
141 temperature and stored then at 4ºC for 24h to achieve the maximum
142 polysaccharide hydration, as reported previously by Camino, Pérez, & Pilosof
143 (2009).

144 **2.3 Turbidity measurement**

145 The turbidity was measured with a turbidimeter device (VELP Scientifica TB1,
146 Italy) at 37ºC. The light source was an infrared emitting diode with a wave length

147 of 850nm. The instrument was calibrated previously with the corresponding
148 standard solutions.

149 OA solubilization: The first measurement was done in SIF (100ml) and then
150 the turbidity was determined after stepwise addition of OA (50μl). OA
151 solubilization was assured by mixing the corresponding sample with an orbital
152 shaker during 5 minutes at 37ºC before the measurement of turbidity. The
153 existence of oiling-off was evidenced after standing the system 48 hours at 37ºC.
154 This procedure was made by duplicate.

155 OA solubilization in the presence of emulsifiers: The same procedure was
156 carried out by duplicate in SIF (100ml) containing the emulsifier (0.5% w/w).

157 **2.4 Particle size determination**

158 In order to analyze the supramolecular assemblies occurring upon the
159 stepwise addition of OA, the particle size distribution was determined by dynamic
160 light scattering (DLS). A Zetasizer Nano-ZS analyzer with a He-Ne laser beam
161 (633 nm) (Malvern Instruments, UK) was used, at a fixed scattering angle of 173º.
162 All the measurements were made at 37ºC. The instrument's measurement range
163 is 0.6 to 6000 nm. By fitting the correlation function with Contin algorithm, a plot
164 of the relative intensity of the light scattered by particles of different sizes was
165 obtained (intensity size distribution). The intensity distribution was converted into
166 the volume size distribution by using the Mie theory (Farías, Martinez, & Pilosof,
167 2010).

168 The assay was performed in duplicate on two individual samples.

169 **3. Results & Discussion**

170 **3.1 Oleic acid solubilization**

171 First of all, the impact of OA addition on turbidity as related to the
172 supramolecular assemblies formed, was studied.

173 The stepwise addition of OA increased turbidity as shown in Fig.1. Two regions
174 could be identified in the curve. In the first region (between 0 and 350μL added
175 OA), the turbidity increased almost linearly. During the second region (above
176 350μL added OA) a steeper increase in turbidity may be observed. In order to
177 understand this behavior, the size of particles was determined by DLS.

178 The analyses of the intensity and volume size distributions of the particles (Fig.
179 2A and 2B) demonstrated that in the first region, OA was present as vesicle
180 (Cistola et al., 1988) that increased in size upon OA addition. When 50μL of OA
181 was added, a monomodal size distribution was observed with a main peak at
182 275nm. With further OA addition, a broader size distribution appeared and the
183 peak shifted to a higher value of 375 nm (for 250μL of OA). An important structural
184 change was apparent when incorporating 350μL of OA, as a bimodal size
185 distribution was observed that correlated with a break point in the turbidity curve
186 (Fig. 1). The lower size peak at 468 nm could be related with the population of
187 vesicles that were increasing in size, as described above. The other population
188 was twice in size (870 nm), indicating that at this point the vesicles began to fuse
189 each other. In agreement with the present results, Zakir, Vaidya, Goyal, Malik, &
190 Vyas (2010) obtained OA vesicles ranging in between 500 nm and 1μm, with a
191 high polidispersity index, measured by DLS. Verma et al. (2013) also obtained
192 OA vesicles with size between 455-554 nm.

193 Above the break point (at 350μL OA), a monomodal size distribution appeared
194 again (Fig. 2A and 2B), but in this case, only the larger particles were present
195 (ranged between 700 and 900 nm). Moreover, oiling off was evidenced 48h after

196 standing the system at 37°C, because all the OA that was added after the break
197 point separated as an upper immiscible phase or droplets phase. This behavior
198 suggests that the limit of solubility of OA was reached. Thus, the second region
199 observed (350 to 600μL) in the turbidity profile, started when the system was
200 saturated by OA. Other authors have reported that the vesicular phase of OA is
201 characterized by an almost flat slope in the absorbance profile and, when droplets
202 appeared, a markedly increase in the absorbance values was observed and a
203 separated oil phase was evidenced (Apel, Deamer, & Mautner, 2002; Rendón et
204 al., 2012; Roy, Mandal, Banerjee, & Sarkar, 2018). These findings are in
205 agreement with the turbidity behavior (first and second region, Fig.1) described
206 before.

207 It can be concluded that the aqueous phase can solubilize 350μL of OA, thus,
208 the OA solubility was 3.13 mg OA/ mL, being the vesicles the predominant
209 supramolecular assemblies. The impact of different food emulsifiers in the
210 solubility and supramolecular assembly of the OA are studied in the following
211 section.

212 **3.2 Oleic acid solubilization in the presence of Tween 80**

213 Tween 80 derivates from the chemical combination of polyethoxylated sorbitan
214 and oleic acid (Karjiban, Basri, Rahman, & Salleh, 2012). In aqueous solution,T80
215 monomers tend to form micelles when reaching the critical micelle concentration
216 (CMC), that is 0.0025% (Gomes, Costa, & Cunha, 2018; Rehman et al., 2017).
217 The driving force for micellization is the hydrophobic effect, which excludes from
218 water the hydrophobic moieties to the interior of the micelle (Karjiban et al., 2012).
219 The volume size distribution of T80 micelles (at 0.5 and 1.5% w/w) was
220 determined in SIF a previous work (Naso, Bellesi, Pizones Ruiz-Henestrosa, &

Pilosof, 2018) where a monomodal particle size distribution was obtained, with a peak at 7.5nm. Other authors have reported similar values for the hydrodynamic diameter of T80 micelles. Lafitte, Thuresson, Jarwoll, & Nydén (2007) obtained a hydrodynamic diameter of 11.4 nm at a concentration of 5% w/w in water. Bhattacharjee et al.(2010) reported a hydrodynamic diameter of 12.2 nm in the presence of 0.4 M NaCl. The lower hydrodynamic diameter obtained in SIF (7.5nm) is consistent with the higher ionic strength of SIF, as the addition of electrolytes may dehydrate hydrophilic groups of the nonionic surfactant (Naso et al., 2018).

The stepwise addition of OA to the solution containing 0.5% w/w T80, gives rise to the turbidity as shown in Fig. 1A. Analyzing this profile, three different regions could be detected, depending on the volume of added OA. In the first region (between 0 and 350μL of OA), the turbidity of the system remained almost constant with very low values. In the second one (between 350 and 550μL of OA) an almost linear increase in the turbidity was observed. A third region (above 600μL of OA) was observed, with a steep increase in the turbidity. To understand how the presence of T80 micelles affected the OA solubility, the size of the particles was analyzed by DLS. The intensity and volume size distribution of the supramolecular assemblies formed, as a function of the amount of added OA, are shown in Fig.3A and 3B, respectively.

When 50μL of OA were added to the solution containing T80 0.5% w/w, a monomodal size distribution was obtained, with a peak at 13 nm. This size was much lower than that corresponding to OA vesicles (275 nm) in the absence of emulsifier (Fig.2). The particle size of 13 nm is consistent with that reported previously by Naso et al. (2018) for T80 micelles. When more OA was

incorporated to the system (from 50 to 350μL), a continuous increase in the mixed micelles sizes up to 40 nm was observed (Fig.3). This behavior reflects that the higher the amount of OA that was incorporated into the T80 micelles, the greater their hydrodynamic diameter. These micellar structures correspond to the first region of the turbidity curve (Fig. 1A) where the turbidity values remain low and almost constant.

Moreover, T80 has molecular similarities with the OA, because it contains an OA molecule in its chemical structure. For that reason, it could be possible that the OA may present affinity for this surfactant, and then it would prefer, instead of rearrange as a vesicle, to get inserted and solubilized in the T80 micelles, enlarging their sizes.

The formation of mixed micelles between T80 and other surfactants has been widely investigated and reported in the literature. Bhattacharjee et al.(2010), Haque et al. (1999), Naso et al. (2018) and Poša et al. (2013) demonstrated the formation of mixed micelles between T80 and different types of bile salts (anionic biological surfactant). Other authors have developed mixed micelles between soybean phospholipids and T80, with a monomodal particles size distribution that presented a peak between 7-20 nm and a low polidispersity index (Liang, Yang, Deng, Lu, & Chen, 2011; Peng et al., 2011). Furthermore, Bhattacharya & Dixit (2015) and Cirin et al. (2011) evidenced the existence of synergism between different types of polysorbates (Tween 20, Tween 40 and Tween 80) and sodium dodecyl sulfate (SDS) with the formation of mixed micelles. They found that the SDS-T80 binary system showed the stronger synergistic effect, because T80 have the longer and more hydrophobic tail, which interacts strongly with the hydrophobic parts of SDS. These findings highlight the capacity of T80 to form

271 mixed micelles with different kinds of surfactants and point out their good
272 compatibility.

273 A break point in the turbidity profile (Fig. 1A) was evidenced at the end of the
274 first region (350μl of OA), where the turbidity values started to increase. This
275 increment could be correlated with the change observed in the particle size
276 distribution in Fig. 3A, where a bimodal population was obtained. The second
277 population could be considered insignificant in the volume size distribution (Fig.
278 3B), but nevertheless, scattered significantly light (Fig. 3A), affecting the turbidity
279 profile.

280 After the break point, in the range of 350 to 600μL added OA, the turbidity of
281 the system started to grow rapidly and linearly (second region). This behavior
282 correlates with the DLS results shown in Fig. 3A, as the population of particles
283 corresponding to T80-OA mixed micelle remained stable, but now, the second
284 population (140nm) scattered more light, increasing the turbidity values in this
285 range. Even though these aggregates coexisted with the mixed micelles, the last
286 ones still predominated according to the volume distribution. With this technique,
287 it was not possible to determine the structure of the second population of
288 particles, but they might be mixed aggregates with more OA than T80.

289 Finally, in the last region (addition of more than 600μl of OA), a change in the
290 slope of the turbidity curve was clearly evidenced, presenting a close relationship
291 with the formation of larger structures of 400 and 5500 nm in the DLS
292 measurements (Fig. 3). The peak at 400 nm seems to be the second population
293 of particles described above (140nm) which increased in size, as more OA was
294 incorporated. On the other hand, the third population at 5500 nm, could
295 correspond to the appearance of a droplet phase, since oiling off was evidenced

296 after 48hs of standing the sample at 37°C. Moreover, a marked increase in the
297 absorbance of the system is related with the formation of OA droplets (Apel et al.,
298 2002; Rendón et al., 2012).

299 Overall, these results indicate that T80 system could solubilize 550μL of OA
300 where 350μL of this volume (first region) could be incorporated into de T80
301 micelles (forming mixed micelles), and the other 200μL (second region), would
302 form mixed structures between both components, probably enriched in OA
303 molecules. Finally, if more than 550μL of OA is added, it cannot be solubilized
304 and the saturation of the system is reached. All the OA added above this point
305 would be separated from the aqueous phase as an upper immiscible phase (third
306 region). Thus, the solubility of OA in this system was 4.92 mg OA/mL. Therefore,
307 it seems that the presence of T80 modifies the original supramolecular assembly
308 of OA (vesicles) improving its solubility in SIF by 57%, suggesting an important
309 affinity between both components.

310 Mirgorodskaya et al. (2010) reported that systems based on micelle forming
311 compounds (Tyloxapol, Triton-X-100, and Brij-97) increased the solubility of FA
312 by more than an order of magnitude compared with water because of the
313 formation of mixed micelles. FA incorporated into micelles increased their size
314 and provoked morphological changes. The solubilization of FA was accompanied
315 by the complete or partial destruction of intrinsic FA aggregates.

316

317 **3.3 Oleic acid solubilization in the presence of β-lactoglobulin**

318 β-lactoglobulin (βlg) is a milk whey protein widely used as an emulsifier and
319 stabilizer agent in food emulsions (Pilosof, 2017).At neutral pH, βlg exists in a
320 dynamic equilibrium between its dimeric and monomeric form (Verheul,

321 Pedersen, Roefs, & De Kruif, 1999). Protein concentration, pH, ionic strength,
322 and temperature affect this equilibrium and, consequently, the proportion of
323 monomers and dimers in solution (Gottschalk, Nilsson, Roos, & Halle, 2003;
324 Sakurai & Goto, 2002). The volume size distribution of βlg (at 0.5 and 1.5% w/w)
325 in SIF was determined in a previous work (Naso et al. 2018). A monomodal
326 particle size distribution was obtained, with a maximum value at 4.6 nm, which
327 falls in between those corresponding to the monomeric (3.6 nm) and the dimeric
328 form (6.9 nm) (Blake, Amin, Qi, Majumda, & Lewis, 2015).

329 The turbidity profile of a solution containing 0.5% w/w βlg, during the stepwise
330 addition of OA, is shown in Fig.1B. Three different regions could be identified
331 taking into account the turbidity curve of the system without emulsifier (included
332 in Fig.1B) and the particles size distributions as more OA is added (Fig.4). In the
333 first region (between 0 and 150μL of OA), the turbidity of the system was lower
334 than that without emulsifier (only SIF). Considering the DLS results in Fig.4, it can
335 be seen that the population of particles that predominated in this region
336 corresponded to βlg particles of 5-6 nm (Naso et al., 2018) and the vesicular
337 structures that OA formed in the absence of emulsifiers (Fig. 2) were not present.
338 This means that the protein included OA within its structure, that is consistent
339 with the role of βlg as a carrier of hydrophobic molecules (Le Maux, Bouhallab,
340 Giblin, Brodkorb, & Croguennec, 2014; Yang et al., 2008). In aqueous solution at
341 neutral pH, βlg forms a flattened and conical barrel, called a calyx (Brownlow et
342 al., 1997; Le Maux et al., 2014; Papiz et al., 1986). It has been demonstrated that
343 this protein in the calyx can bind hydrophobic ligands, such as, fatty acids, retinol,
344 vitamin D, cholesterol, aromatic molecules, polyphenols and many others
345 compounds (Fang, Zhang, Tian, & Ren, 2015; Kanakis et al., 2011; Le Maux,

346 Giblin, Croguennec, Bouhallab, & Brodkorb, 2012; Lišková et al., 2011; Loch et
347 al., 2013; O'neill & Kinsella, 1988; Papiz et al., 1986; Puyol, Perez, Peiro, &
348 Calvo, 2010; Wang, Allen, & Swaisgood, 2010a). In spite of being the calyx the
349 main binding site, a second binding site in the dimer interface has been proposed
350 (Kontopidis, Holt, & Sawyer, 2010; Loch et al., 2013; Wang, Allen, & Swaisgood,
351 2010b; Yang et al., 2008).

352 In the case of the FA-βlg binding, it has been proposed that may serve to
353 enhance the delivery of the FA to the enterocyte, improving its bioaccessibility
354 (Le Maux et al., 2012; Puyol et al., 2010). On the other hand, Lišková et al.(2011)
355 obtained a complex between βlg and sodium oleate (the salt of OA) and they
356 demonstrated that this complex could induce apoptosis in cancer cells, having
357 antitumor activity. Also, Fang et al.(2015) prepared a βlg-OA complex that
358 exhibited the same cytotoxicity towards tumors cells. By isothermal titration
359 calorimetry (ITC), they confirmed that OA interacts with the protein through van
360 der Waals and hydrogen bonds. Similarly, Loch et al.(2013) evidenced by ITC the
361 same type of interactions between βlg and the OA and showed that the binding
362 was spontaneous and exothermic. Furthermore, Salama, Foda, Hassan, & Awad
363 (2015) in a series of works, obtained different nanocomplexes between other
364 whey proteins (α-lactalbumin and whey protein isolate) and OA. By turbidity
365 measurements, they confirmed the existing interactions, as all the complexes
366 showed lower turbidity values compared to the OA alone. This could be attributed
367 to the presence of the protein which decreased the ability of the OA to aggregate
368 in solution, demonstrating the higher binding ability of the proteins (Hassan et al.,
369 2014; Salama et al., 2015). These results correlate very well with the turbidity
370 behavior of the βlg system studied in this work (Fig.1B).

371 Taking into account all these considerations, the second region in the turbidity
372 profile started with a break point at 150μL and extended up to 350μL of added
373 OA (Fig. 1B). In this region the turbidity values were still lower than the system
374 without the protein, indicating that the OA was bound to the protein and did not
375 self-assembled as vesicles. Moreover, in the volume particle size distribution (Fig.
376 4B) a bimodal population of particles appeared (for 250μL of OA), with one peak
377 at 18 nm and the other at 114 nm. At this point, the structure corresponding to
378 βlg dimmer (6 nm) disappeared, probably because the binding sites for the OA
379 were saturated. The molecules of OA and βlg rearranged to give place to new
380 types of supramolecular assemblies (18 nm and 114 nm) that could still maintain
381 the OA solubilized in the aqueous phase.

382 In the third region (above 350μL of added OA), the turbidity curve of the
383 solution containing βlg was almost similar to that without it shown as a reference
384 in Fig. 1B. The DLS results (Fig.4) indicated that the population of particles with
385 a mean size of 18 nm disappeared, and the peak corresponding to the mixed OA-
386 βlg aggregates at 114nm became broader and polydisperse (120 nm). It seems
387 that the system evolved to the supramolecular assembly of 120 nm as more OA
388 was added. In this way, these particles were enriched of OA as has been
389 postulated for the T80 system (Fig. 3). In addition, a new population of aggregates
390 at 4000 nm appeared, that could be related with the formation of OA droplets,
391 since oiling off was evidenced after 48 hs of standing the sample at 37°C,
392 indicating that the system reached the saturation limit.

393 By considering these results, it can be concluded that βlg could solubilize
394 350μL of OA, where 150μL of this volume was bound within the protein structure
395 (first region), and the other 200μL (second region), could remain in the aqueous

396 phase forming mixed structures between both components (Fig.6). Finally, when
397 adding more OA (third region) droplets emerged, and an upper immiscible phase
398 was formed after 48h. Thus, the OA solubility in this system was 3.13 mg OA/
399 mL. It is important to highlight that in the presence of βlg the same amount of OA
400 was solubilized than in the reference system; however, in the presence of the
401 protein, OA was not present as vesicles, but formed lower supramolecular
402 assemblies.
403

404 **3.4 Oleic acid solubilization in the presence of HPMC**

405 Hydroxypropylmethylcellulose (HPMC) is a family of surface active
406 polysaccharides derived from cellulose. They containmethyl (hydrophobic) and
407 hydroxypropyl (hydrophilic) groups in the anhydroglucose backbone of the
408 cellulose and, depending on the degree of substitution, they differ in their
409 physico-chemical properties and technological applications (Pizones Ruiz-
410 Henestrosa, Bellesi, Camino, & Pilosof, 2017).

411 In the turbidity profile of solution containing HPMC (0.5% w/w) (Fig.1B), two
412 different regions could be identified during the stepwise addition of OA, according
413 to the DLS results. In order to better understand the turbidity behavior, the
414 turbidity curve of the system without HPMC was also included in Fig. 1B as a
415 reference. The particle size distribution of the HPMC solution was determined to
416 assess the aggregation behavior of the polysaccharide in the absence of OA (Fig.
417 5). In the intensity size distribution, a bimodal population (peaks at 17 nm and
418 271 nm) could be observed (Fig. 5A). However, only the lower size population
419 was significant, according to the volume size distribution, indicating that most of
420 the particles were ranged in this size. Camino et al. (2009) and Pizones Ruiz-

421 Henestrosa et al. (2017) reported a similar particle size distribution for the same
422 HPMC (E5LV) in water. It has been reported that the HPMC molecules tend to
423 self-associate in aqueous solutions and form aggregates or clusters, being the
424 size of the aggregates concentration-dependent (Camino et al., 2009; Pizones
425 Ruiz-Henestrosa et al., 2017). It seems that the self-assembly of HPMC
426 molecules could be driven by hydrophobic interactions between the hydrophobic
427 substituents (Kato, Yokoyama, & Takahashi, 1978). In this case, two types of
428 HPMC clusters of different mean size particles were present (17 and 271 nm),
429 but those with smaller size predominated (Fig. 5B). It could be possible that the
430 biggest aggregates resulted from the self-association of the smallest.

431 In the first region (between 0 and 350μL of OA) of the turbidity profile (Fig. 1B),
432 the turbidity of the HPMC system was lower than the reference, as observed for
433 the protein system described above. Considering the DLS results (Fig.5), in this
434 case, a population of large particles appeared in both size distributions (intensity
435 and volume), with a wide and polydispersed peak at 317 nm. The original
436 predominating HPMC cluster of 17 nm disappeared and possibly these small
437 clusters tended to self-associate to form particles of bigger size, in the presence
438 of the OA. The inclusion of the OA molecules in the clusters gave rise to a mixed
439 structure of larger size (317 nm). As more OA was incorporated (from 0 to 350μL),
440 the size of the HPMC-OA mixed particles shifted to bigger sizes (Fig.5), indicating
441 the increasing inclusion of OA in the clusters structure. In this region, the turbidity
442 of the system was always lower than the system with OA alone (Fig.1B), pointing
443 out that the OA would be bound to the polysaccharide clusters and OA vesicles
444 would not be formed.

445 On the other hand, in the second region (above 350μL of added OA), the
446 turbidity curve of the HPMC system crossed the turbidity curve of the reference
447 (Fig.1B). The DLS results indicated that when 350μL of OA were incorporated to
448 the system, the mixed HPMC-OA clusters reached their biggest size (532 nm),
449 and from this point, as more OA was added, the size of the particles did not
450 change (Fig. 5). Nevertheless, a new population of 4500 nm appeared, that could
451 be related with the formation of OA droplets, since oiling off was evidenced after
452 48h of standing the sample at 37°C. All these observations may indicate that the
453 system reached the FA saturation limit when adding 350μL of OA.

454 Overall, these results suggest that the HMPC system could solubilize 350μL
455 of OA, the same amount than the βlg system. However, in this case, the OA
456 remained in the aqueous phase through its inclusion in the polysaccharide
457 clusters (Fig.6). Thus, the OA solubility in this system was 3.13 mg OA/ mL,
458 Moreover, comparing with the reference system (without HPMC), the HPMC
459 solution could disperse the same amount of OA, nevertheless the FA adopted a
460 supramolecular assembly different from vesicles in the presence of this
461 polysaccharide.

462

463 **4. Conclusions**

464 The combined assessment of the changes in turbidity, oiling off and the
465 supramolecular structures of OA by DLS allowed the determination of the
466 solubilization extent of OA.

467 Figure 6 summarizes the possible supramolecular assemblies that could be
468 formed between OA and the different emulsifiers as function of the amount of OA.
469 Our results indicated that T80 improved by 57% the solubilization of OA, whereas

the macromolecules (βlg and HPMC) only affected the supramolecular structure that OA adopted in solution, being not more as a vesicle.

The methodology described here opens the possibility to assess FA solubility in a variety of systems of practical application in the food, pharmacy and nutritional fields, as the assessment of the potential accessibility of FA during *in vitro* lipolysis. In this sense, although the emulsifier nature is known to impact in the kinetic of lipolysis of an emulsion, there is a lack of understanding of the specific mechanisms that govern this effect. The influence of the emulsifier nature on the FA solubility is a possible mechanism that could be involved.

Acknowledgements

This work has been supported by Universidad de Buenos Aires (Grant Number 20020130100524), Consejo Nacional de Investigaciones Científicas y Técnicas, Agencia Nacional de Promoción Científica y Tecnológica (Grant Number: PICT-2014-3668).

References

Apel, C. L., Deamer, D. W., & Mautner, M. N. (2002). Self-assembled vesicles of monocarboxylic acids and alcohols: Conditions for stability and for the encapsulation of biopolymers. *Biochimica et Biophysica Acta - Biomembranes*, *1559*(1), 1–9. https://doi.org/10.1016/S0005-2736(01)00400-X

Bellesi, F. A., Pizones Ruiz-Henestrosa, V. M., & Pilosof, A. M. R. (2014). Behavior of protein interfacial films upon bile salts addition. *Food Hydrocolloids*, *36*, 115–122. https://doi.org/10.1016/j.foodhyd.2013.09.010

Bhattacharjee, J., Verma, G., Aswal, V. K., Date, A. A., Nagarsenker, M. S., & Hassan, P. A. (2010). Tween 80-sodium deoxycholate mixed micelles: Structural characterization and application in doxorubicin delivery. *Journal of Physical Chemistry B*, *114*(49), 16414–16421. https://doi.org/10.1021/jp108225r

Bhattacharya, M., & Dixit, S. G. (2015). Study of mixed micelles of Sodium dodecyl sulphate and nonionic surfactants polysorbates tween series : Their interaction and thermodynamic parameter using cyclic voltammetry, *3*(3), 22–25.

Blake, S., Amin, S., Qi, W., Majumda, M., & Lewis, E. N. (2015). Colloidal stability & conformational changes in β-lactoglobulin: Unfolding unfolding to self-assembly. *International Journal of Molecular Sciences*, *16*(8), 17719–17733. https://doi.org/10.3390/ijms160817719

Brownlow, S., Morais Cabral, J. H., Cooper, R., Flower, D. R., Yewdall, S. J., Polikarpov, I., … Sawyer, L. (1997). Bovine β-lactoglobulin at 1.8 Å resolution - Still an enigmatic lipocalin. *Structure*, *5*(4), 481–495. https://doi.org/10.1016/S0969-2126(97)00205-0

Camino, N. A., Pérez, O. E., & Pilosof, A. M. R. (2009). Molecular and functional modification of hydroxypropylmethylcellulose by high-intensity ultrasound. *Food Hydrocolloids*, *23*(4), 1089–1095. https://doi.org/10.1016/j.foodhyd.2008.08.015

Camino, N. A., Sánchez, C. C., Rodríguez Patino, J. M., & Pilosof, A. M. R.

(2011). Hydroxypropylmethylcellulose at the oil-water interface. Part I. Bulk behaviour and dynamic adsorption as affected by pH. *Food Hydrocolloids*, *25*(1), 1–11. https://doi.org/10.1016/j.foodhyd.2010.04.012

Chen, I. A., & Szostak, J. W. (2004). A kinetic study of the growth of fatty acid vesicles. *Biophysical Journal*, *87*(2), 988–998. https://doi.org/10.1529/biophysj.104.039875

Cirin, D., Posa, M., Krstonosic, V., & Milanovic, M. (2011). Conductometric study of sodium dodecyl sulfate - nonionic surfactant (Triton X-100, Tween 20, Tween 60, Tween 80 or Tween 85) mixed micelles in aqueous solution. *Hemijska IndustrijaChemical Industry*, *66*(1), 21–28. https://doi.org/10.2298/hemind110612059c

Cistola, D. P., Hamilton, J. A., Jackson, D., & Small, D. M. (1988). Ionization and Phase Behavior of Fatty Acids in Water: Application of the Gibbs Phase Rule. *Biochemistry*, *27*(6), 1881–1888. https://doi.org/10.1021/bi00406a013

de Kruijff, B., Killian, J. A., Staffhorst, R., van Santen, R. A., Hilbers, P. A. J., Pfleger, N., & Markvoort, A. J. (2010). Self-Reproduction of Fatty Acid Vesicles: A Combined Experimental and Simulation Study. *Biophysical Journal*, *99*(5), 1520–1528. https://doi.org/10.1016/j.bpj.2010.06.057

Fang, B., Zhang, M., Tian, M., & Ren, F. Z. (2015). Self-assembled β-lactoglobulin–oleic acid and β-lactoglobulin–linoleic acid complexes with antitumor activities. *Journal of Dairy Science*, *98*(5), 2898–2907. https://doi.org/10.3168/jds.2014-8993

Farías, M. E., Martinez, M. J., & Pilosof, A. M. R. (2010). Casein glycomacropeptide pH-dependent self-assembly and cold gelation.

International Dairy Journal, *20*(2), 79–88. https://doi.org/10.1016/j.idairyj.2009.09.002

Freeman, C. P. (1969). Properties of fatty acids in dispersions of emulsified lipid and bile salt and the significance of these properties in fat absorption in the pig and the sheep. *British Journal of Nutrition*, *23*(02), 249. https://doi.org/10.1079/bjn19690032

Gomes, A., Costa, A. L. R., & Cunha, R. L. (2018). Impact of oil type and WPI/Tween 80 ratio at the oil-water interface: Adsorption, interfacial rheology and emulsion features. *Colloids and Surfaces B: Biointerfaces*, *164*, 272–280. https://doi.org/10.1016/j.colsurfb.2018.01.032

Gottschalk, M., Nilsson, H., Roos, H., & Halle, B. (2003). Protein self-association in solution: The bovine β -lactoglobulin dimer and octamer. *Protein Science*, *12*(11), 2404–2411. https://doi.org/10.1110/ps.0305903

Haque, M. E., Das, A. R., & Moulik, S. P. (1999). Mixed micelles of sodium deoxycholate and polyoxyethylene sorbitan monooleate (Tween 80). *Journal of Colloid and Interface Science*, *217*(1), 1–7. https://doi.org/10.1006/jcis.1999.6267

Hassan, Z., Awad, R., El-sayed, M., Foda, M., Otzen, D., & Salama, H. (2014). Interaction between whey protein nanoparticles and fatty acids. *Integrative Food, Nutrition and Metabolism*, *1*(2), 91–97. https://doi.org/10.15761/IFNM.1000107

Hofmann, A. F. (1963). the Function of Bile Salts in Fat Absorption. the Solvent Properties of Dilute Micellar Solutions of Conjugated Bile Salts. *The Biochemical Journal*, *89*(1953), 57–68. Retrieved from http://www.ncbi.nlm.nih.gov/pubmed/14097367%0Ahttp://www.pubmedcent

570 ral.nih.gov/articlerender.fcgi?artid=PMC1202272

571 Kanakis, C. D., Hasni, I., Bourassa, P., Tarantilis, P. A., Polissiou, M. G., &
572 Tajmir-Riahi, H. A. (2011). Milk β-lactoglobulin complexes with tea
573 polyphenols. *Food Chemistry*, *127*(3), 1046–1055.
574 https://doi.org/10.1016/j.foodchem.2011.01.079

575 Karjiban, R. A., Basri, M., Rahman, M. B. A., & Salleh, A. B. (2012). Structural
576 Properties of Nonionic Tween80 Micelle in Water Elucidated by Molecular
577 Dynamics Simulation. *APCBEE Procedia*, *3*(May), 287–297.
578 https://doi.org/10.1016/j.apcbee.2012.06.084

579 Kato, T., Yokoyama, M., & Takahashi, A. (1978). Melting temperatures of
580 thermally reversible gels IV. Methyl cellulose-water gels. *Colloid and*
581 *Polymer Science Kolloid Zeitschrift & Zeitschrift Für Polymere*, *256*(1), 15–
582 21. https://doi.org/10.1007/BF01746686

583 Kontopidis, G., Holt, C., & Sawyer, L. (2010). Invited Review: β-Lactoglobulin:
584 Binding Properties, Structure, and Function. *Journal of Dairy Science*,
585 *87*(4), 785–796. https://doi.org/10.3168/jds.s0022-0302(04)73222-1

586 Lafitte, G., Thuresson, K., Jarwoll, P., & Nydén, M. (2007). Transport properties
587 and aggregation phenomena of polyoxyethylene sorbitane monooleate
588 (polysorbate 80) in pig gastrointestinal mucin and mucus. *Langmuir*,
589 *23*(22), 10933–10939. https://doi.org/10.1021/la701081s

590 Le Maux, S., Bouhallab, S., Giblin, L., Brodkorb, A., & Croguennec, T. (2014).
591 Bovine β-lactoglobulin/fatty acid complexes: Binding, structural, and
592 biological properties. *Dairy Science and Technology*, *94*(5), 409–426.
593 https://doi.org/10.1007/s13594-014-0160-y

594 Le Maux, S., Giblin, L., Croguennec, T., Bouhallab, S., & Brodkorb, A. (2012).

β-Lactoglobulin as a molecular carrier of linoleate: Characterization and effects on intestinal epithelial cells in vitro. *Journal of Agricultural and Food Chemistry*, *60*(37), 9476–9483. https://doi.org/10.1021/jf3028396

Liang, H., Yang, Q., Deng, L., Lu, J., & Chen, J. (2011). Phospholipid-Tween 80 mixed micelles as an intravenous delivery carrier for paclitaxel. *Drug Development and Industrial Pharmacy*, *37*(5), 597–605. https://doi.org/10.3109/03639045.2010.533276

Lišková, K., Auty, M. A. E., Chaurin, V., Min, S., Mok, K. H., O'Brien, N., … Brodkorb, A. (2011). Cytotoxic complexes of sodium oleate with β-lactoglobulin. *European Journal of Lipid Science and Technology*, *113*(10), 1207–1218. https://doi.org/10.1002/ejlt.201100109

Loch, J. I., Bonarek, P., Polit, A., Riès, D., Dziedzicka-Wasylewska, M., & Lewiński, K. (2013). Binding of 18-carbon unsaturated fatty acids to bovine β-lactoglobulin-Structural and thermodynamic studies. *International Journal of Biological Macromolecules*, *57*, 226–231. https://doi.org/10.1016/j.ijbiomac.2013.03.021

Maldonado-Valderrama, J., Wilde, P., MacIerzanka, A., & MacKie, A. (2011). The role of bile salts in digestion. *Advances in Colloid and Interface Science*, *165*(1), 36–46. https://doi.org/10.1016/j.cis.2010.12.002

Minekus, M., Alminger, M., Alvito, P., Ballance, S., Bohn, T., Bourlieu, C., … Brodkorb, A. (2014). A standardised static in vitro digestion method suitable for food-an international consensus. *Food and Function*, *5*(6), 1113–1124. https://doi.org/10.1039/c3fo60702j

Mirgorodskaya, A. B., Yatskevich, E. I., & Zakharova, L. Y. (2010). The solubilization of fatty acids in systems based on block copolymers and

nonionic surfactants. *Russian Journal of Physical Chemistry A*, *84*(12), 2066–2070. https://doi.org/10.1134/S0036024410120101

Naso, J. N., Bellesi, F. A., Pizones Ruiz-Henestrosa, V. M., & Pilosof, A. M. R. (2018). Studies on the interactions between bile salts and food emulsifiers under in vitro duodenal digestion conditions to evaluate their bile salt binding potential. *Colloids and Surfaces B: Biointerfaces*, *174*(November 2018), 493–500. https://doi.org/10.1016/j.colsurfb.2018.11.024

O'neill, T., & Kinsella, J. E. (1988). Effect of Heat Treatment and Modification on Conformation and Flavor Binding by β-Lactoglobulin. *Journal of Food Science*, *53*(3), 906–909. https://doi.org/10.1111/j.1365-2621.1988.tb08982.x

Papiz, M. Z., Sawyer, L., Eliopoulos, E. E., North, A. C. T., Findlay, J. B. C., Sivaprasadarao, R., … Kraulis, P. J. (1986). The structure of β-lactoglobulin and its similarity to plasma retinol-binding protein. *Nature*, *324*(6095), 383–385. https://doi.org/10.1038/324383a0

Parker, R., Rigby, N. M., Ridout, M. J., Gunning, A. P., & Wilde, P. J. (2014). The adsorption-desorption behaviour and structure function relationships of bile salts. *Soft Matter*, *10*(34), 6457–6466. https://doi.org/10.1039/c4sm01093k

Peng, X., Wang, K., Zhang, X., Geng, H., Bao, C., Cui, D., … Wang, J. (2011). Development of Polysorbate 80/Phospholipid mixed micellar formation for docetaxel and assessment of its in vivo distribution in animal models. *Nanoscale Research Letters*, *6*(1), 354. https://doi.org/10.1186/1556-276x-6-354

Pilosof, A. M. R. (2017). Potential impact of interfacial composition of proteins

and polysaccharides stabilized emulsions on the modulation of lipolysis. The role of bile salts. *Food Hydrocolloids*, *68*, 178–185. https://doi.org/10.1016/j.foodhyd.2016.08.030

Pizones Ruiz-Henestrosa, V. M., Bellesi, F. A., Camino, N. A., & Pilosof, A. M. R. (2017). The impact of HPMC structure in the modulation of in vitro lipolysis: The role of bile salts. *Food Hydrocolloids*, *62*, 251–261. https://doi.org/10.1016/j.foodhyd.2016.08.002

Poša, M., Ćirin, D., & Krstonošić, V. (2013). Physico-chemical properties of bile salt-Tween 80 mixed micelles in the viewpoint of regular solution theory. *Chemical Engineering Science*, *98*, 195–202. https://doi.org/10.1016/j.ces.2013.05.042

Puyol, P., Perez, M. D., Peiro, J. M., & Calvo, M. (2010). Effect of Binding of Retinol and Palmitic Acid to Bovine β-Lactoglobulin on Its Resistance to Thermal Denaturation. *Journal of Dairy Science*, *77*(6), 1494–1502. https://doi.org/10.3168/jds.s0022-0302(94)77088-0

Rasi, S. (2003). Regulation of Size Distribution in Fatty Acid and Mixed Phospholipid/Fatty Acid Vesicles.

Rehman, N., Ullah, H., Alam, S., Jan, A. K., Khan, S. W., & Tariq, M. (2017). Surface and thermodynamic study of micellization of non ionic surfactant/diblock copolymer system as revealed by surface tension and conductivity. *Journal of Materials and Environmental Science*, *8*(4), 1161–1167.

Rendón, A., Carton, D. G., Sot, J., García-Pacios, M., Montes, R., Valle, M., … Ruiz-Mirazo, K. (2012). Model systems of precursor cellular membranes: Long-chain alcohols stabilize spontaneously formed oleic acid vesicles.

670 *Biophysical Journal*, *102*(2), 278–286.
671 https://doi.org/10.1016/j.bpj.2011.12.026
672 Roy, S., Mandal, S., Banerjee, P., & Sarkar, N. (2018). Modification of fatty acid
673 vesicle using an imidazolium-based surface active ionic liquid: a detailed
674 study on its modified properties using spectroscopy and microscopy
675 techniques §. *Journal of Chemical Sciences*, *130*(10), 1–14.
676 https://doi.org/10.1007/s12039-018-1532-2
677 Sakurai, K., & Goto, Y. (2002). Manipulating monomer-dimer equilibrium of
678 bovine β-lactoglobulin by amino acid substitution. *Journal of Biological*
679 *Chemistry*, *277*(28), 25735–25740. https://doi.org/10.1074/jbc.M203659200
680 Salama, H. H., Foda, M., Hassan, Z. M. R., & Awad, R. A. (2015). Characteristic
681 and cytotoxic activity of different α -Lactalbumin / fatty acids nanocomplex,
682 (February).
683 Sarkar, A., Ye, A., & Singh, H. (2016). On the role of bile salts in the digestion of
684 emulsified lipids. *Food Hydrocolloids*, *60*, 77–84.
685 https://doi.org/10.1016/j.foodhyd.2016.03.018
686 Shu, X., Meng, Y., Wan, L., Li, G., Yang, M., & Jin, W. (2014). pH-Responsive
687 Aqueous Foams of Oleic Acid/Oleate Solution. *Journal of Dispersion*
688 *Science and Technology*, *35*(2), 293–300.
689 https://doi.org/10.1080/01932691.2013.785363
690 Small, D. M. (1986). *The Physical Chemistry of Lipids: From Alkanes to*
691 *Phospholipids* (1st ed.). Springer.
692 Smith, A., & Lough, A. K. (1976). Micellar solubilization of fatty acids in aqueous
693 media containing bile salts and phospholipids. *The British Journal of*
694 *Nutrition*, *35*(1), 77–87.

Tzocheva, S. S., Kralchevsky, P. A., Danov, K. D., Georgieva, G. S., Post, A. J., & Ananthapadmanabhan, K. P. (2012). Solubility limits and phase diagrams for fatty acids in anionic (SLES) and zwitterionic (CAPB) micellar surfactant solutions. *Journal of Colloid and Interface Science*, *369*(1), 274–286. https://doi.org/10.1016/j.jcis.2011.12.036

Verheul, M., Pedersen, J. S., Roefs, S. P. F. M., & De Kruif, K. G. (1999). Association behavior of native β-lactoglobulin. *Biopolymers*, *49*(1), 11–20. https://doi.org/10.1002/(SICI)1097-0282(199901)49:1<11::AID-BIP2>3.0.CO;2-1

Verkade, P. E., & Meerburg, W. (1955). The solubility of some normal saturated fatty acids in an aqueous sodium glycocholate solution. *Recueil Des Travaux Chimiques Des Pays-Bas*, *74*(3), 263–270. https://doi.org/10.1002/recl.19550740302

Verma, S., Bhardwaj, A., Vij, M., Bajpai, P., Goutam, N., & Kumar, L. (2013). Oleic acid vesicles : A new approach for topical delivery of antifungal agent Oleic acid vesicles : a new approach for topical delivery of antifungal agent, (May). https://doi.org/10.3109/21691401.2013.794351

Walde, P., Namani, T., Morigaki, K., & Hauser, H. (2010). Formation and Properties of Fatty Acid Vesicles (Liposomes). *Liposome Technology, Volume I*, (April 2014), 1–19. https://doi.org/10.1201/9780849397264.ch1

Wang, Q., Allen, J. C., & Swaisgood, H. E. (2010a). Binding of Vitamin D and Cholesterol to β-Lactoglobulin. *Journal of Dairy Science*, *80*(6), 1054–1059. https://doi.org/10.3168/jds.s0022-0302(97)76030-2

Wang, Q., Allen, J. C., & Swaisgood, H. E. (2010b). Protein Concentration Dependence of Palmitate Binding to β-Lactoglobulin. *Journal of Dairy*

720 *Science*, *81*(1), 76–81. https://doi.org/10.3168/jds.s0022-0302(98)75553-5

721 Yang, M. C., Guan, H. H., Liu, M. Y., Lin, Y. H., Yang, J. M., Chen, W. L., …
722 Mao, S. J. T. (2008). Crystal structure of a secondary vitamin D 3 binding
723 site of milk β-lactoglobulin. *Proteins: Structure, Function and Genetics*,
724 *71*(3), 1197–1210. https://doi.org/10.1002/prot.21811

725 Zakir, F., Vaidya, B., Goyal, A. K., Malik, B., & Vyas, S. P. (2010). Development
726 and characterization of oleic acid vesicles for the topical delivery of
727 fluconazole. *Drug Delivery*, *17*(4), 238–248.
728 https://doi.org/10.3109/10717541003680981

729
730
731
732
733
734
735
736
737
738

739

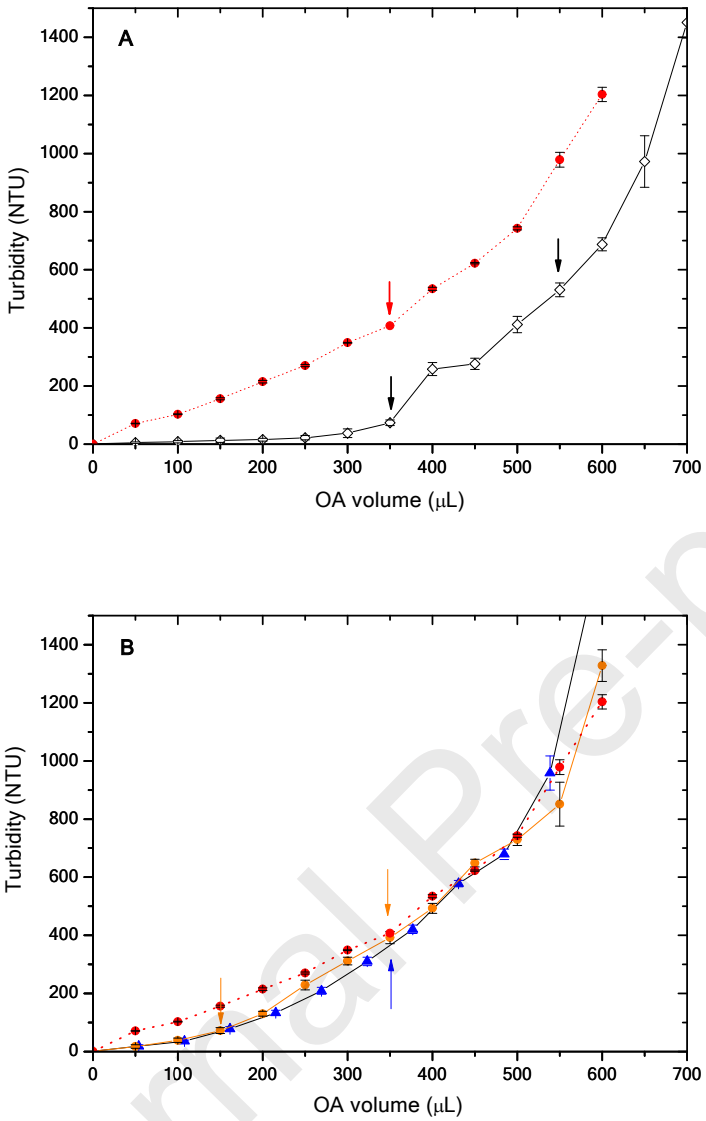

740

741

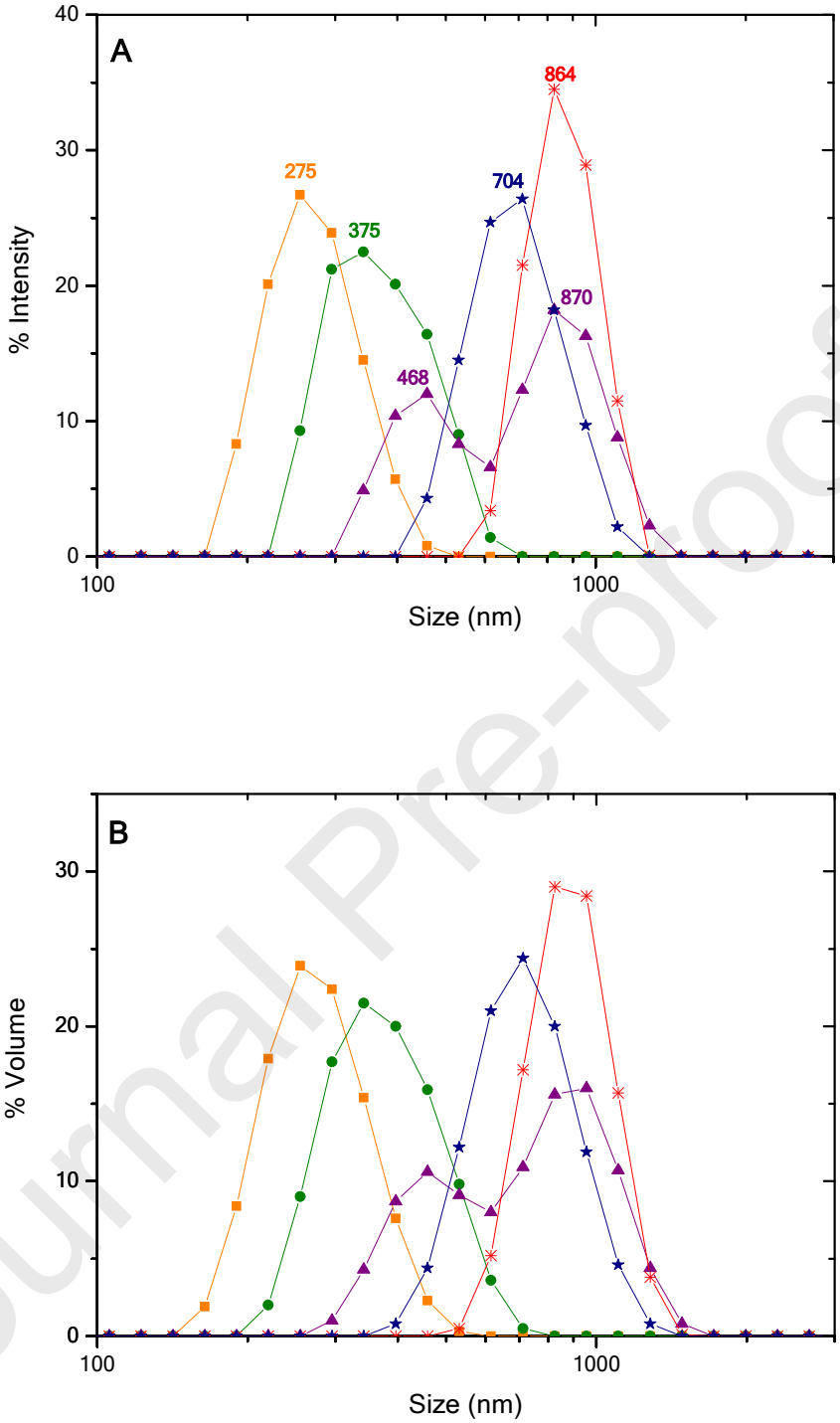

742

743

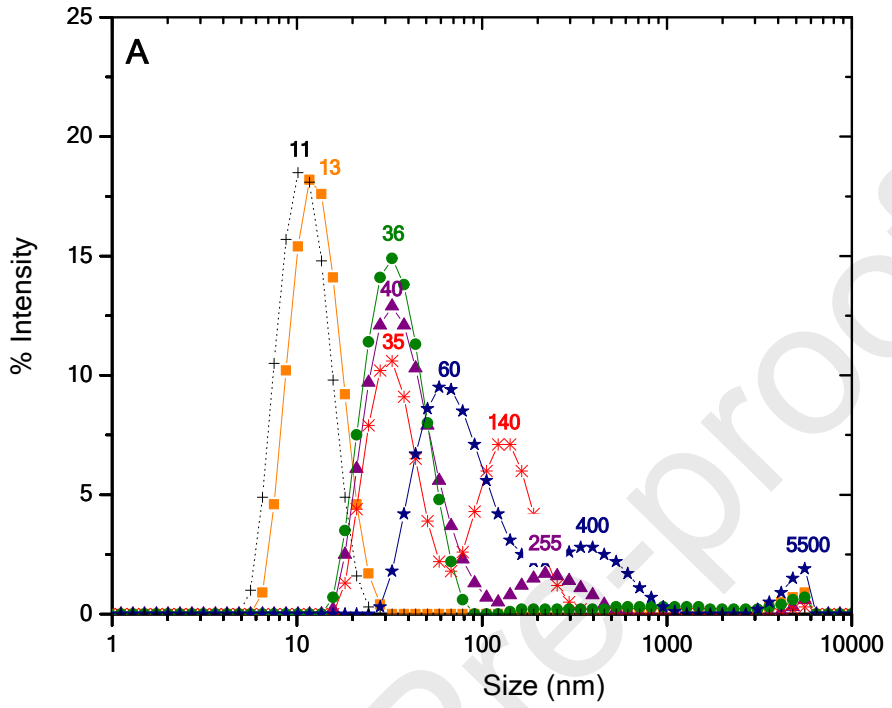
A
% Intensity
Size (nm)
11
13
36
40
35
60
140
255
400
5500

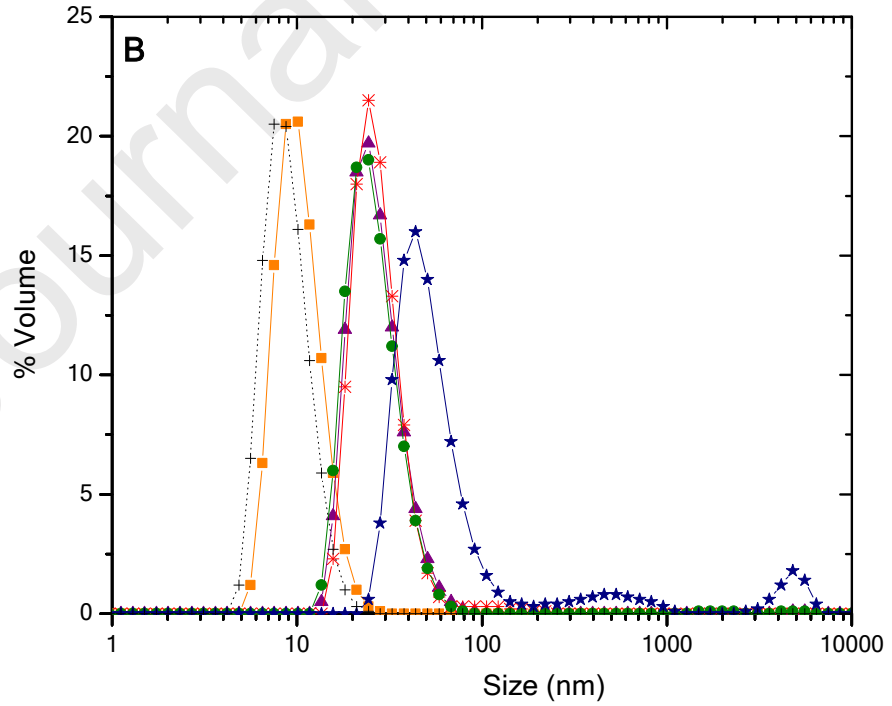
B
% Volume
Size (nm)

744

745

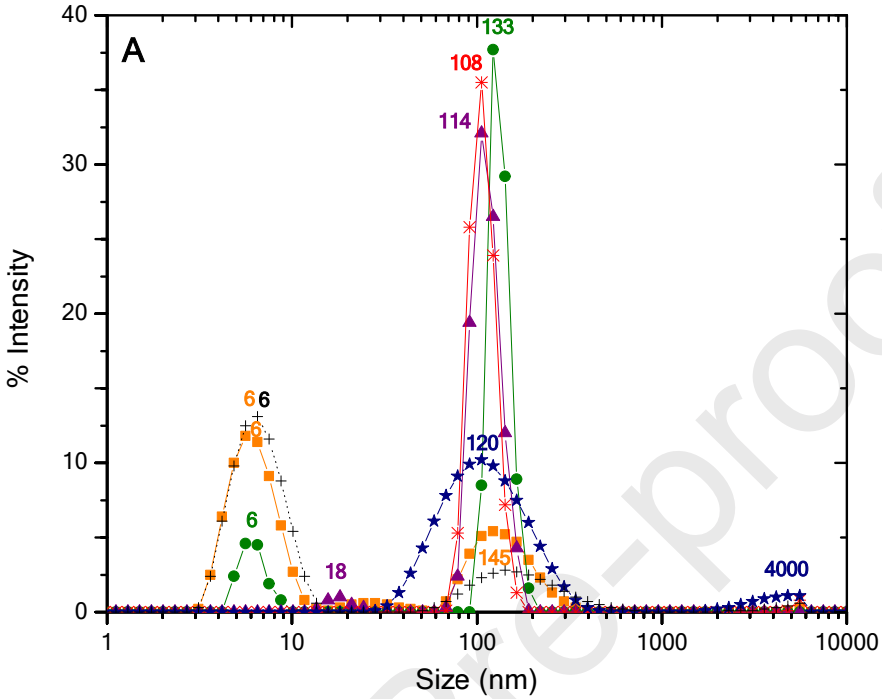
A
% Intensity
Size (nm)
133
108
114
6
6
6
6
120
18
145
4000

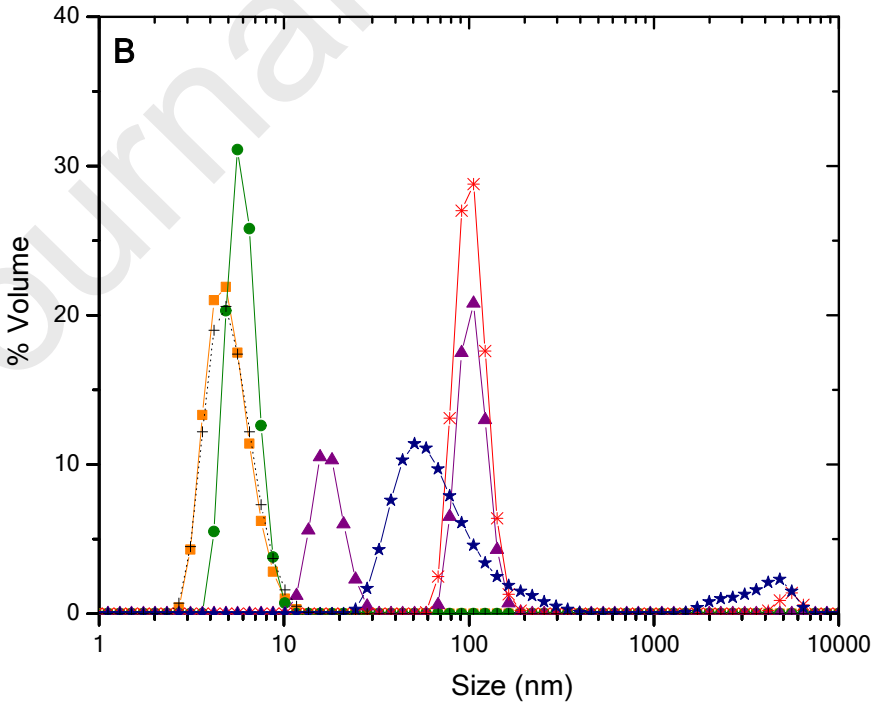
B
% Volume
Size (nm)

746

747

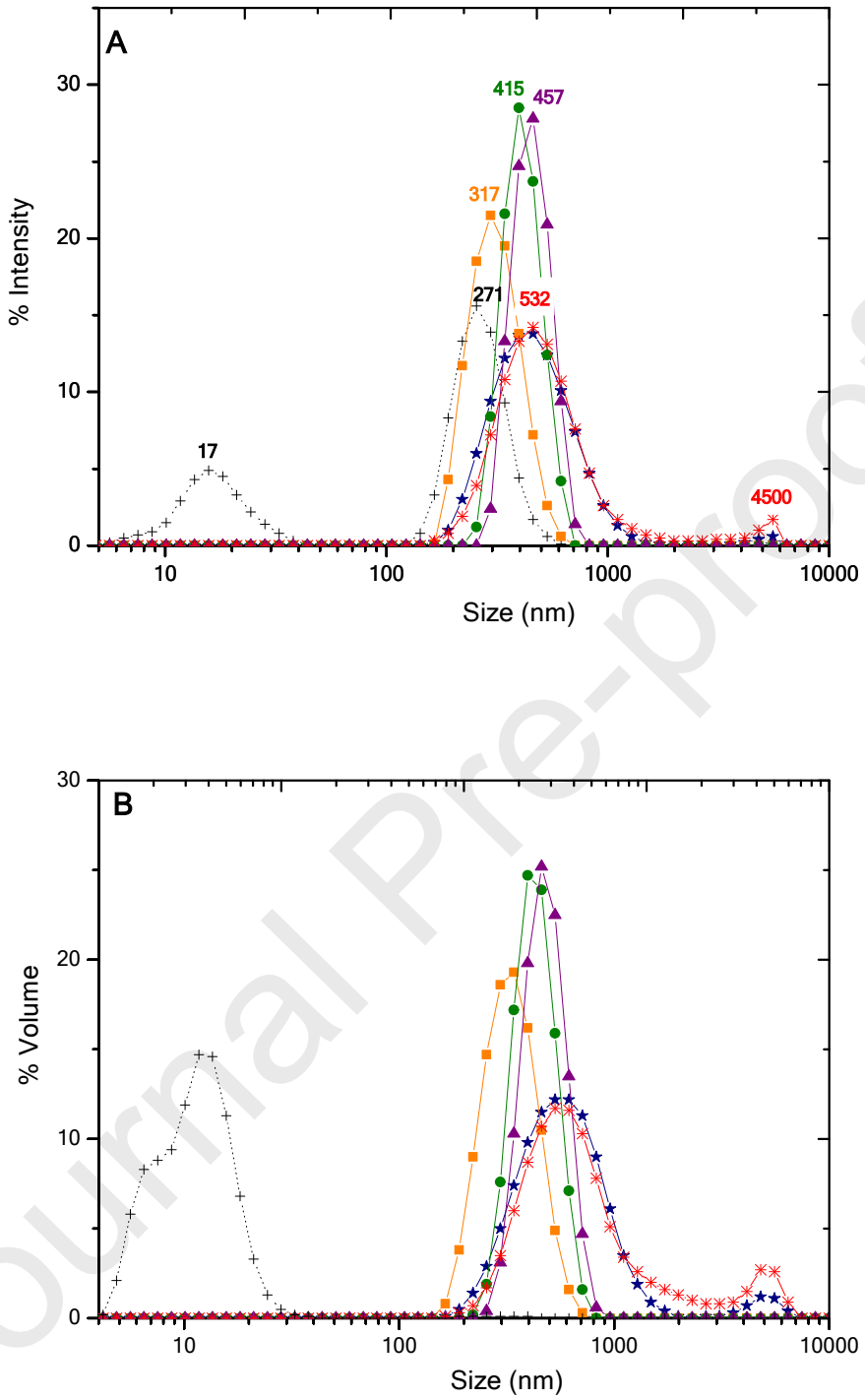

748

749

Error! Not a valid embedded object.

Fig.1 Turbidity evolution of SIF upon the stepwise addition of OA in the presence of low (A) and high (B) molecular weight emulsifiers (0.5% w/w). Tween 80 (◊), βlg (●), HPMC (▲). Turbidity profile of the reference system (without emulsifier) (--●--). The limits between the different regions were indicated with arrows.

Fig.2 Changes of the particles size distribution of OA in the absence of emulsifier when adding: 50µL (■), 250µL (●), 350µL (▲), 450µL (✳) and 600µL (☆) of OA. Size distribution as function of intensity (A) and volume (B).

Fig.3 Changes of the particles size distribution of OA in the presence of T80 (0.5% w/w) when adding: 50µL (■), 250µL (●), 350µL (▲), 450µL (✳) and 700µL (☆) of OA. T80 system (0.5% w/w) without OA (+). Size distribution as function of intensity (A) and volume (B).

Fig.4 Changes of the particles size distribution of OA in the presence of βlg (0.5% w/w) when adding: 50µL (■), 150µL (●), 250µL (▲), 350µL (✳) and 600µL (☆) of OA. βlg system (0.5% w/w) without OA (+). Size distribution as function of intensity (A) and volume (B).

Fig.5 Changes of the particles size distribution of OA in the presence of HPMC (0.5% w/w) when adding: 50µL (■), 150µL (●), 250µL (▲), 350µL (✳) and 550µL (☆) of OA. HPMC system (0.5% w/w) without OA (+). Size distribution as function of intensity (A) and volume (B).

Fig.6 Schematic representation of the possible supramolecular assemblies that could be formed between the OA and the different emulsifiers in SIF as a function of the amount of OA. OA without emulsifiers (A), OA in presence of T80 (B), OA in presence of βlg (C) and OA in presence of HPMC (D)

Graphical abstract

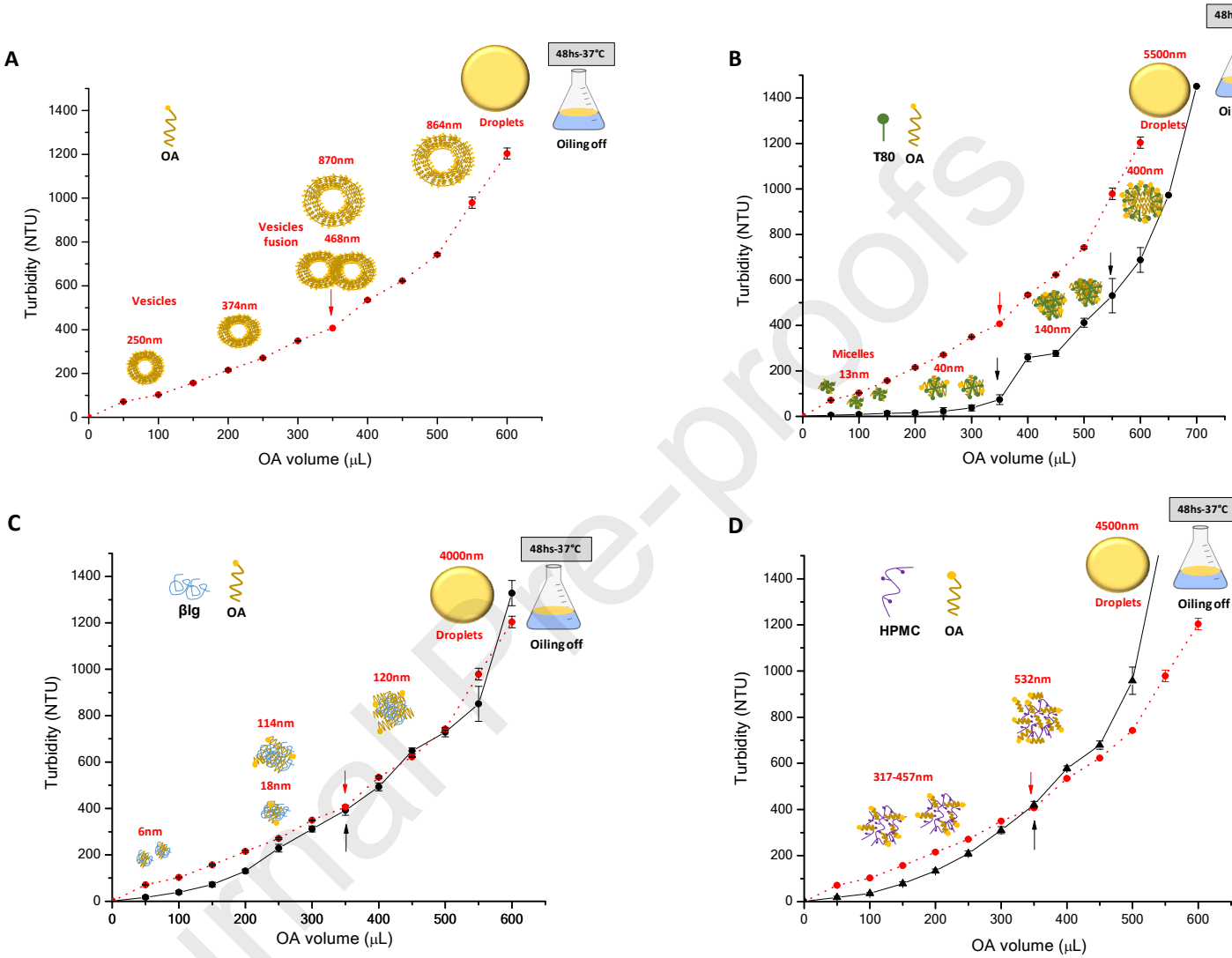

785 **HIGHLIGHTS**

786 The methodology allowed to determine the solubility of a FA

787 The presence of T80 improved the solubilization of OA

788 The macromolecules affected the supramolecular structure that the OA adopt

789

790

791

792

Credit autorship contribution statament:

Julieta N Naso: Methodology, investigation, validation, writing-review & editing

Fernando A Bellesi: Methodology, investigation, validation, writing-review & editing

Victor M Pizones Ruiz-Henestrosa: Methodology, writing-review & editing, supervision, project administration, funding acquisition

Ana M R Pilosof: Conceptualization, methodology, writing-review & editing project , supervision, administration, funding acquisition